J. Farm Sci., 38(1): (23-28) 2025

RESEARCH PAPER

Analysis of land use land cover of Vijayapura taluk using remote sensing and GIS techniques

SHANKAR GOUD C. PATIL[1], S. B. PATIL[1*], R. A. NANDAGAVI[1] AND M. S. SHIRAHATTI[2]

[1]Department of Agronomy, [2]Department of Agril Engineering, College of Agriculture, Vijayapura - 586 101
University of Agricultural Sciences, Dharwad - 580 005, India
*E-mail: patilsb13617@uasd.in

(Received: August, 2024 ; Accepted: January, 2025)

DOI: doi.org/10.61475/JFS.2025.v38i1.05

Abstract: The dynamic transformation of land use and land cover (LULC) has become a crucial aspect of effective natural resources management and continuous environmental monitoring. A research study utilizing remote sensing (RS) and geographic information system (GIS) techniques was conducted in Vijayapura Taluk, Vijayapura District, Karnataka during 2023-24 to analyze LULC changes. Remote sensing has proven to be a useful tool for generating LULC maps and identifying and quantifying crop areas. The objective of this study was to classify and map the LULC of the study area using RS and GIS techniques A supervised classification was performed using the maximum likelihood classification algorithm in the Semi-Automatic Classification Plugin (SCP) of QGIS software. Sentinel-2 satellite images captured on May 1 and December 1, 2023, were analyzed to estimate LULC changes between *summer* to *rabi* seasons. In the *summer* season, water bodies constituted 0.63 per cent, vegetation covered 25.05 per cent, built-ups/habitat comprised 6.67 per cent and bare land made up 67.65 per cent of the total study area. In contrast, during the *rabi* season, water bodies slightly increased to 0.66 per cent, vegetation significantly rose to 69.65 per cent, built-ups/habitat expanded to7.52 per cent and bare land decreased to 22.16 per cent. These results highlight a substantial increase in vegetation cover during the *rabi* season compared to the *summer* season, emphasizing the importance of rainfall and residual soil moisture for crop cultivation, along with a corresponding reduction in bare land. The accuracy assessment of LULC classification revealed an overall accuracy of 90.45 per cent for *summer* and 89.44 per cent for *rabi*, with kappa coefficients of 0.87 and 0.84, respectively, demonstrating the reliability of the classification method.

Key words: GIS, QGIS, SCP, Sentinel-2, Vegetation cover

Introduction

Remote sensing (RS) refers to the science and practice of acquiring information about an object, area, or phenomenon by analyzing data captured by a device that remains distant from the subject being investigated (Lilles and Kiefer, 2009). This technique holds the promise of providing quantitative, instantaneous and non-destructive insights into land use land cover (LULC) over expansive areas. Its integration with image analysis technology opens up access to planetary-scale spatial information, laying the foundation for LULC analysis.These strides are attributable to the growing adoption of innovative technologies that monitor spatial and temporal changes in land use. Remote sensing technology emerges as a pivotal player in the success of LULC analysis, working in tandem with other technologies such as the Internet of Things (IoT), robotic systems, weather forecasting, and global positioning systems (GPS).The integration of remote sensing technology with other state-of-the-art innovations has paved the way for more sustainable practices by providing timely and accurate information on Earth's features and agricultural phenomena.

LULC describes the type of human activities or natural features present in a specific area (Kassawmar *et al.,* 2016). Temporal models of LULC changes are crucial for analyzing the causes and patterns of land use transformations (Lin *et al*., 2008). LULC classification is utilized across various fields, including agriculture (Gibril *et al*., 2016), environmental management (Jiang *et al*., 2015), and urban expansion (Wang and Maduako, 2018).The LULC is vital because it gives data, which can beused as input for modelling, especially, one dealing with the environment, for instance, models deal with climate change and policy developments (Hudait and Patel, 2022). LULC has been mapped from different sources like geographical maps, soil study associations, statistical data and so on; yet these are helpful for explicit purposes only and are not truly reliable. However, with the advent of remote sensing technology, every one of these issues has been cleared out, beating allthe restrictions and has led to the speedy portrayal of the real world in the most ideal manner. Keeping all these things in mind a research study was conducted in Vijayapura taluk of Vijayapura district, Karnataka to analyse the LULC change during 2023.

Material and methods

Geographical information of the study area

The experiment was conducted in Vijayapura taluk of Vijayapura district, Karnataka state in India. It is situated at 16° 45′ 36″ to 17° 02′ 24″ North latitude and 75° 34′ 48″ to 76° 05′ 24″ East longitude and at a mean elevation of 670 meters above mean sea level. The physiography ofthe whole area is gently sloping, ranging from 1 to 5 per cent from west to east and it falls under the Northern Dry Zone of Karnataka (Zone-3) (Fig. 1).

Equipment, image data and software used for the investigation

The integration of remote sensing and GIS techniques provides reliable information about land use land cover (LULC) changes. Garmin GPS receiver was used for recording the location details such as latitude and longitude of different land use classes. The Sentinel-2 (S2) images, developed by the

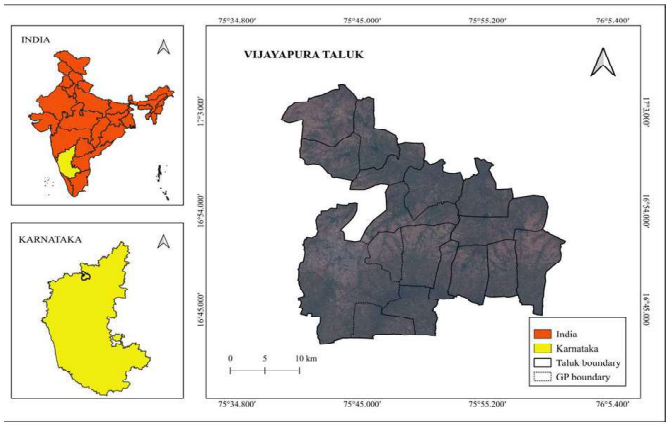

Fig 1. Study area map

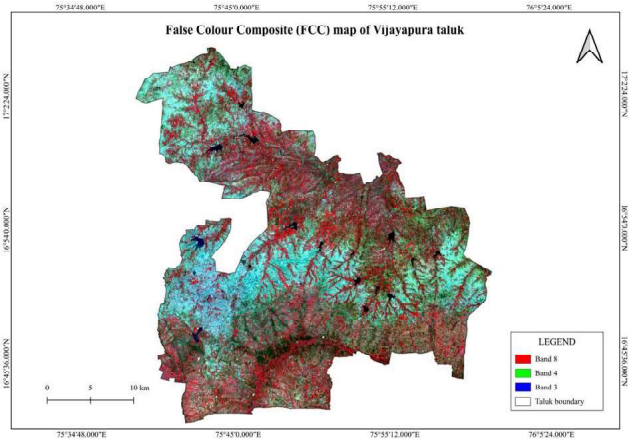

Fig 2. False colour composite (FCC) map of study area

European Space Agency (ESA), having high resolution and frequent revisit capabilities were utilized for LULC analysis.These images are freely available in the Copernicus data space ecosystem browser and were downloaded for two dates May 01 and December 01, 2023 and used for LULC analysis. A QGIS install was developed from the OSGeo4W and it is available on the official website for download. It includes these additional packages: GDAL, Orfeo Tool Box, QGIS and Python. The QGIS 3.32.3 software was downloaded and used for the classification, analysis, mapping and accuracy assessment of classified data. The downloaded S2 images were loaded in QGIS where, the red filter was given to near-infrared (NIR), the green filter to red and the blue filter to the green band to get the false colour composite (FCC) image of the study area (Fig. 2).

Generation of LULC map of the study area

Land cover mapping primarily involves categorizing satellite images using supervised classification techniques. This method

Table 1. The ground truth details of different land use classes used as training sites in the study area

Land use class	Latitude (DMS)	Longitude (DMS)	Land use class	Latitude (DMS)	Longitude (DMS)
Waterbodies	16º44'45.80"	75º45'03.40"	Vegetation	16º42'56.9"	75º46'48.9"
	16º43'13.20"	75º45'58.30"		16º42'54.0"	75º46'53.1"
	16º44'35.90"	75º49'29.00"		16º43'01.6"	75º47'21.1"
	16º46'45.60"	75º48'55.40"		16º43'05.0"	75º48'51.8"
	16º49'14.70"	75º50'37.30"		16º43'06.8"	75º49'09.6"
	16º50'37.30"	75º49'10.50"		16º45'00.0"	75º50'13.7"
	16º53'05.50"	75º42'52.60"		16º45'10.9"	75º50'01.8"
	16º47'59.20"	75º42'38.10"		16º48'07.5"	75º50'46.0"
Built-ups/ Habitat	16º50'04.87"	75º44'36.57"		16º48'16.5"	75º51'39.5"
	16º51'17.96"	75º42'38.22"		16º49'41.7"	75º51'11.2"
	16º44'58.90"	75º45'00.30"		16º46'04.9"	75º44'32.6"
	16º43'05.00"	75º48'19.30"		16º43'19.0"	75º49'22.6"
	16º44'07.30"	75º50'07.40"		16º45'44.9"	75º43'23.74"
	16º46'57.90"	75º48'50.30"		16º44'12.1"	75º49'55.6"
	16º49'39.80"	75º50'54.10"		16º42'57.2"	75º46'57.3"
	16º45'23.16"	75º43'53.60"		16º43'01.6"	75º47'21.1"
	16º47'56.08"	75º43'32.63"		16º43'00.1"	75º48'11.4"
	16º48'0.99"	75º43'54.79"		16º43'02.0"	75º48'03.2"
	16º45'59.23"	75º44'43.44"		16º43'04.8"	75º48'34.6"
Bare land	16º42'59.60"	75º47'05.70"		16º43'49.4"	75º49'53.7"
	16º43'09.60"	75º49'13.30"		16º44'09.9"	75º49'58.8"
	16º49'42.20"	75º50'35.50"		16º45'01.9"	75º50'09.5"
	16º49'19.30"	75º45'49.10"		16º45'27.0"	75º49'48.2"
	16º52'13.69"	75º43'16.32"		16º47'59.3"	75º50'34.6"
	16º45'48.44"	75º44'55.11"		16º48'22.0"	75º51'34.6"
	16º44'37.84"	75º45'03.64"		16º49'03.4"	75º51'48.0"
	16º44'56.00"	75º44'52.74"		16º49'42.8"	75º50'06.5"
	16º46'25.43"	75º43'20.86"		16º46'19.22"	75º43'20.12"
	16º46'39.95"	75º43'18.19"		16º53'05.50"	75º42'52.60"
	16º46'48.37"	75º43'16.33"		16º47'59.20"	75º42'38.10"

DMS- Degree Minute and Seconds

Table 2. Land cover classification scheme

Macro class ID	Macro class name	Micro class
1	Waterbodies	Farm ponds, ponds, lakes, rivers, streams and swamps
2	Vegetation	Lands covered with agricultural and horticultural crops, pastures, trees, garden vegetation and shrubs.
3	Built-ups/ Habitat	Land covered by buildings and other man-made structures *viz*., Residential, commercial services, industrial area, mixed urban or built-up area as roads *etc*.,
4	Bare land	Lands with exposed soil, sand or rocks, bare ground, bare exposed rocks, strip mines, quarries, gravel pits and fallow during *kharif* which were cultivated during *rabi* season.

requires user input to define the specific land cover classes of interest. The location details of different land use classes were collected with the help of a Gramin GPS receiver (Table 1) and are used as user input. In this study, the ESA's (European Space Agency) Sentinel-2 (S2) images were used for mapping LULC in the Semi-Automatic Classification Plugin (SCP) of QGIS.

LULC mapping is based on the analysis of S2 images acquired on May 01 and December 01, 2023 of the major crops' grand growth stages to improve the spectral discrimination between classes of natural and cultivated vegetation. Fig. 3 depicts the general workflow of LULC analysis.

For the digital S2 image analysis, SCP, an open-source plugin developed by Luca Congedo that enables the implementation

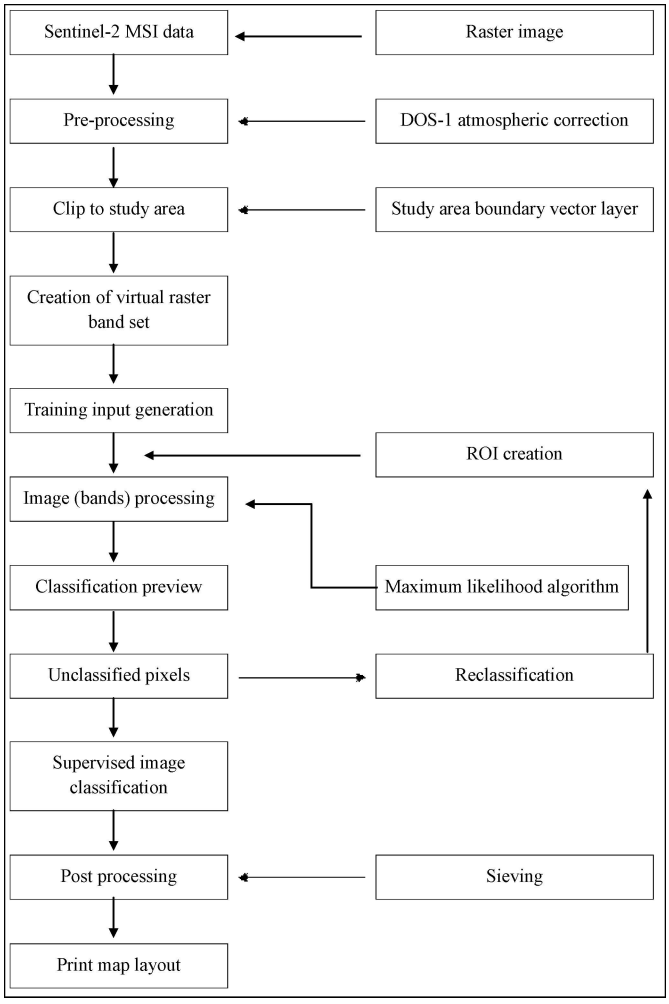

Fig 3. Work flow for LULCmapping using SCP in QGIS

of Semi-Automatic Classification was installed through the official repository of QGIS plugins. Pre-processing operations are necessary before initiation of the classification process.These operations serve to harmonize data when it originates from diverse sensors and/or acquisition time frames.

The process of converting data to surface reflectance is crucial for S2 imagery. Initially provided as Top of Atmosphere (TOA) data, a transformation to Top of Canopy (TOC) reflectance is necessary. To accomplish this the SCP's atmospheric correction technique known as DOS1 (Dark Object Subtraction) applied to the image. Then clipping of the S2 image over the study area was performed. This was done by selecting all the bands of S2 images and clipping them by using clip by mask layer of the raster analysis menu of QGIS by specifying no data values as "0". After these spectral bands are clipped, get converted into TOC, the last pre-processing step consists of creating a group of layers or a multiband image containing all the bands required for the classification process, it also called a "band set". It was necessary to create a single dataset from the set of initial bands. This step also made it possible to display combinations of bands or colour composite images (True colour and FCC) to facilitate visual discrimination of the different elements in the image.

Processing operations include the supervised classification and accuracy assessment. In supervised classification, we seek to group pixels according to their spectral resemblance to reference objects representative of the land cover classes and defined a priori by the user. This includes several sub-steps,the creation of training sites [Region of Interest (ROI)] which was made to build a training database to train the determine rules of discrimination between the different land cover classes. The macro class ROI created during this study were waterbodies, vegetation, built-ups/ habitat and bare land (Table 2). This step was followed by classification preview and assessment of spectral signatures, where, it provides the qualitative assessment of the training database quality provided by the classification preview. A classification was created based on the training sites.This preview was done to reduce the risk of confusion between the classes in the final classification. Further, this was followed by the classification step which isconcerned with the extrapolation of the entire image of the previously identified training sites and for which a thematic land cover class could be attributed via a classification algorithm (model). The Maximum likelihood algorithm classifies each object (or pixels) present in the image by comparing its spectral characteristics with those of the reference objects in the training

Table 3. Area covered under different LULC classes of *summer* 2023 as observed from supervised classification of Sentinel -2 image dated May, 01

Class ID	Land use classes	Pixel Sum	Percentage (%)	Area (ha)
1	Waterbodies	60052	0.63	600.52
2	Vegetation	2389408	25.05	23894.08
3	Built-ups/ Habitat	635972	6.67	6359.72
4	Bare land	6452399	67.65	64523.99
	Total	9537831	100	95378.31

database. This was then followed by an assessment of the classification accuracy which is a fundamental step in the process because it allows quantify the quality of the map obtained. For this, the classification was compared with reference data (independent of those used to perform the classification) by means of a confusion matrix. The reference data (or testing sites) were obtained in the same way as the training sites except that here the sites used were to assess theposterior quality of the classification. This new sampling must therefore be representative of the whole image. The confusion matrix allowed to compute different statistics.

The post-processing of image classification involves certain operations as merging of same classes with strong resemblance and filtering of isolated pixels in the final classification as these may have an impact on the accuracy of the classification. A filter (4 and 4) was applied to replace the pixels isolated by the majority class observed in the pixels included in a defined neighbourhood window. This was followed by converting the raster data into vector data in the shape file format.The attribute table of the vector file then has an attribute relating to the LULC classes. This was followed by the final step in the digital image analysis for LULC which is the print map layout.The vectors of classes were exported into the print layout window of QGIS to print the map and added map coordinates, legend, direction indicator and title of the map. Finally, the printed map was exported into *png* format.

Results and discussion

LULC transformation

Land use and land cover transformation from *summer* to *rabi* of 2023 involves the dynamic shift of land features from one form to another over a period of time, caused by either natural events or human-induced activities. (Richards, 1990; Amin and Fazal, 2012). Supervised classification conducted using a maximum likelihood algorithm utilizing Sentinel-2 images to analyze the land use changes from *summer* to *rabi* season of the year 2023 as the study area is located in the Northern Dry Zone (Zone-3), depends mainly on rainfall for agriculture revealed the area distribution under different land use classes. In the *summer*, water bodies accounted for 0.63 per cent, vegetation covered 25.05 per cent, built-ups/ habitat comprised 6.67 per cent and bare land made up 67.65 per cent of total study area (Table 3 and Fig. 4). In the *rabi* season, water bodies constituted 0.66 per cent, vegetation increased to 69.65 per cent, built-ups/ habitat occupied 7.52 per cent and bare land decreased to 22.16 per cent (Table 4 and Fig. 5). This data highlights a significant increase in vegetation coverage during the *rabi* season compared to the *summer* season, indicating substantial crop growth or natural vegetation recovery due to the residual monsoon soil moisture and development of irrigation facility in the study area. There was a corresponding decrease in bare land in *rabi* compared to *summer* reflecting a conversion of previously exposed areas into productive agricultural land. This is because the region is mainly dryland and depends mostly on rainfall for crop production with limited irrigation sources and facilities, especially during *summer*. The built-up areas saw a modest increase from 6.67 to 7.52 per cent, suggesting limited urban growth or infrastructure development and also, there is a probability (proportionate to the errors) that ground reference points for this category were classified incorrectly as urbanization is not this speed in actuality. Lu *et al.* (2003), also found that most of the time, the traditional approach to classification (such as MLC) only distinguishes clearly between forest and non-forest land use and land cover. Water bodies remained relatively stable (0.63 to 0.66%) throughout the year, underscoring their consistent presence despite seasonal changes.

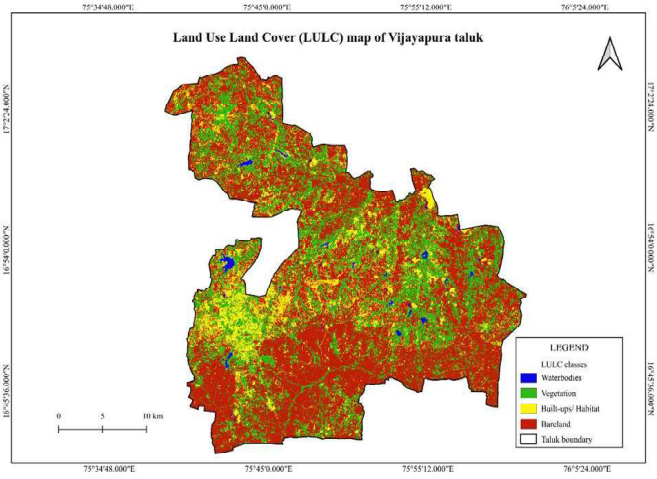

Fig.4. LULC map for *summer* 2023 of the study area

Accuracy assessment

Accuracy assessment is an essential aspect of feature extraction from classified images. It identifies potential error

Table 4. Area covered under different LULC classes of *rabi* 2023 as observed from supervised classification of Sentinel -2 image dated December, 01

Class ID	Land use classes	Pixel Sum	Percentage (%)	Area (ha)
1	Waterbodies	63291	0.66	632.91
2	Vegetation	6643527	69.65	66435.27
3	Built-ups/ Habitat	717398	7.52	7173.98
4	Bare land	2113615	22.16	21136.15
	Total	9537831	100	95378.31

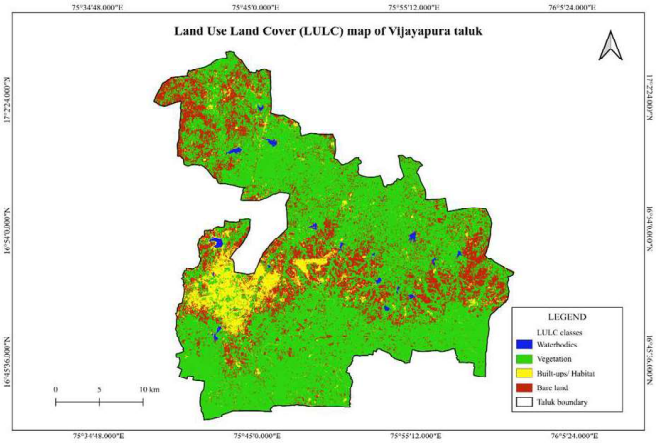

Fig 5. LULC map for *rabi* 2023 of the study area

sources in the classified image, thereby improving the quality of the information derived from the data (Lea and Curtis, 2010).The confusion matrix, also known as the error matrix, is the standard approach used to evaluate the accuracy of a classified image (Onur *et al.,* 2009; Mujabar and Chandrasekar, 2013). This method compares the pixels in the classified image with those in a reference image, where the correct class is already established (Szuster *et al*., 2011). The confusion matrix records pixels of agreement and disagreement by comparing the class and location of each ground truth pixel with its counterpart in the classified image. It is organized as a c x c matrix (where c represents the number of classes), with rows and columns indicating the number of pixels from the test data. In this matrix, the columns represent the pixel count for each class in the reference data, while the rows correspond to the pixel count for each class in the classified image (SCGE, 2011). Using this error matrix, accuracy is evaluated through three metrics: producer's accuracy, user's accuracy and overall accuracy, based on commission and omission errors (Boschetti *et al*., 2004; Carlotto, 2009). Producer's accuracy is calculated by dividing the total number of correctly classified units (pixels) in a specific class (xy) by the total number of class (xy) units (pixels) identified in the reference data (Bradley, 2009; Mohammady *et al*., 2015). In contrast, the user's accuracy is the ratio of correctly classified class (xy) units to the total number of units (pixels) classified as class (xy). Overall accuracy is determined by dividing the sum of all correctly classified units (pixels) by the total number of units (pixels) across all classes (Lu and Weng, 2007; Li and Zhou, 2009). The Kappa coefficient is a metric utilized in image classification to assess the accuracy of classifications, focusing on both the diagonal elements and the overall elements within the confusion matrix. This coefficient is derived from the

Table 5. Confusion matrix derived accuracy indices of different classes of LULC for *summer* 2023

Class ID	Producer's Accuracy (%)	User's Accuracy (%)
1	99.55	96.18
2	91.20	89.42
3	81.22	87.40
4	83.72	86.10

Overall accuracy (%) = 90.45

Kappa hat classification (K_{hat}) = 0.87

Table 6. Confusion matrix derived accuracy indices of different classes of LULC for *rabi* 2023

Class ID	Producer's Accuracy (%)	User's Accuracy (%)
1	100	99.14
2	89.71	83.14
3	87.62	91.27
4	86.11	83.02

Overall accuracy (%) = 89.44

Kappa hat classification (K_{hat}) = 0.84

comparison between the actual agreement observed in the error matrix and the agreement expected by chance, taking into account the total counts in the respective rows and columns (Viera and Garrett, 2005; Foody, 2010).

The accuracy assessment was conducted using 60 samples from various land use classes, with these reference points overlaid onto the classified images to evaluate the accuracy of the feature classification and the results for both *summer* (Table 5) and *rabi* (Table 6) LULC classifications demonstrated a high degree of reliability. The *summer* LULC achieved an overall accuracy of 90.45 per cent, while the *rabi* LULC showed an overall accuracy of 89.44 per cent. These high accuracy levels highlight the effectiveness of the classification process in accurately reflecting land cover conditions. The user's accuracy for *summer* LULC ranged from 86.10 to 96.18 per cent and for *rabi* LULC, it ranged from 83.02 to 99.14 per cent, indicating a precise identification of land cover types. The producer's accuracy, ranging from 81.22 to 99.55 per cent for *summer* LULC and from 86.11 to 100 per cent for *rabi* LULC, further supports the reliability of the classifications in capturing true land cover. The Kappa hat values of 0.87 for *summer* and 0.84 for *rabi* demonstrate strong agreement between the classified data and reference data, validating the consistency of the classifications. These findings suggest that the classification methods used are highly effective and that the resulting LULC maps are a dependable representation of land cover for both seasons. The observed minimal discrepancies in accuracy values across different land cover types reinforce the robustness of the classifications, making them valuable for further analysis and application.

Conclusion

The LULC analysis using Sentinel-2 imagery and supervised classification in QGIS proved to be a highly effective approach for mapping and monitoring of land cover changes in Vijayapura Taluk during *summer* and *rabi* season of 2023.The study demonstrated significant seasonal shifts, with vegetation cover increasing during the *rabi* season due to the influence of rainfall and residual soil moisture, while bare land decreased accordingly. The high overall accuracy (90.45% for *summer* and 89.44% for *rabi*) and kappa values (0.87 and 0.84, respectively) shows the reliability of the classification method.This analysis provides critical insights for natural resource management, sustainable land use practice and urban planning, highlighting the importance of remote sensing and GIS techniques in supporting informed decision-making for environmental and land use management.

References

Amin A and Fazal S, 2012, Land transformation analysis using remote sensing and GIS techniques (A case study). *Journal of Geographic Information System,* 4(3): 229-236.

Bradley B A, 2009, Accuracy assessment of mixed land cover using a GIS-designed sampling scheme. *International Journal of Remote Sensing,* 30(13): 3515-3529.

Boschetti L, Flasse S P and Brivio P A, 2004, Analysis of the conflict between omission and commission in low spatial resolution dichotomic the matic products: the Pare to Boundary. *Remote Sensing of Environment*, 91(3): 280-292.

Carlotto M J, 2009, Effect of errors in ground truth on classification accuracy. *International Journal of Remote Sensing*. 30(18): 4831-4849.

Foody G M, 2010, Assessing the accuracy of land cover change with imperfect ground reference data. *Remote Sensing of Environment*, 114(10): 2271-2285.

Gibril M B A, Bakar S A, Yao K, Idrees M O and Pradhan B, 2016, Fusion of RADARSAT-2 and multispectral optical remote sensing data for LULC extraction in a tropical agricultural area. *Geocarto International*, 32(7): 735-748.

Hudait M and Patel P P, 2022, Crop-type mapping and acreage estimation in small holding plots using Sentinel-2 images and machine learning algorithms: Some comparisons. *The Egyptian Journal of Remote Sensing and Space Science*, 25(1): 147-156.

Jiang L, Li C Y, Song B and LiSS, 2015, Impacts of land use/cover changes on carbon storage in Beijing 1990-2010. *International Journal of Environmental Studies*, 72(6): 972-982.

Kassawmar T, Eckert S, Hurni K, Zeleke G and Hurni H, 2016, Reducing landscape heterogeneity for improved land use and land cover (LULC) classification across the large and complex Ethiopian highlands. *Geocarto International*, 33(1):53-69.

Lea C and Curtis AC, 2010, *Thematic accuracy assessment procedures: National Park Service Vegetation Inventory*. US Department of the Interior, National Park Service, Natural Resource Program Center. Retrieved from http://science.nature.nps.gov/im/inventory/veg/index.cfm

Li B and Zhou Q, 2009, Accuracy assessment on multi temporal land cover change detection using a trajectory error matrix. *International Journal of Remote Sensing*, 30(5): 1283-1296.

Lilles T M and Kiefer R W, 2009, Remote sensing and image interpretation, Textbook of Jain Wiley and Sons, *Asia Private Limited Singapore 6th edition.*

Lin Y P, Wu PJ and Hong N M, 2008, The effects of changing the resolution of land-use modelling on simulations of land-use patterns and hydrology for a watershed land-use planning assessment in Wu-Tu, Taiwan. *Landscape and Urban Planning*, 87(1):54-66.

Lu D and Weng Q, 2007, A survey of image classification methods and techniques for improving classification performance. *International Journal of Remote Sensing*, 28(5):823-870.

Lu D, Moran E and Batistella M, 2003, Linear mixture model applied to Amazonian vegetation classification. *Remote Sensing Environment*, 87: 456-469.

Mohammady M, Moradi H R, Zeinivand H and Temme AJAM, 2015, A comparison of supervised, unsupervised and synthetic land use classification methods in the north of Iran. *International Journal of Environmental Science and Technology*, 12:1515-1526.

Mujabar P S and Chandrasekar N, 2013, Shoreline change analysis along the coast between Kanyakumari and Tuticorin of India using remote sensing and GIS. *Arabian Journal of Geosciences*, 6: 647-664.

Onur I, Maktav D, Sari M and Kemal Sönmez N, 2009, Change detection of land cover and land use using remote sensing and GIS: a case study in Kemer, Turkey. *International Journal of Remote Sensing*, 30(7): 1749-1757.

Richards J F, 1990, Land transformation. *The earth as transformed by human action*, pp.163-178.

SCGE, 2011, Supervised/unsupervised land use land Cover classification using ERDAS imagine. Summer course computational geoecology. Retrieved from http://horizon.science.uva

Szuster BW, Chen Q and Borger M, 2011, A comparison of classification techniques to support land cover and land use analysis in tropical coastal zones. *Applied Geography*, 31(2): 525-532.

Viera A J and Garrett J M, 2005, Understanding interobserver agreement: the kappa statistic. *Family Medicine*, 37(5):360-363.

Wang J and Maduako I N, 2018, Spatio-temporal urban growth dynamics of Lagos Metropolitan Region of Nigeria based on Hybrid methods for LULC modelling and prediction. *European Journal of Remote Sensing*, 51(1): 251-265.